Benchmark on Cu-Ni co-deposition in $CuSO_4/NiSO_4$ solution by a three-dimensional mass transport and electrochemical model

Jaeyeong Park[1*], Sungjun Son[1], Sungyeol Choi[1], Kwang-Rag Kim[2], Il Soon Hwang[1]
[1]Department of Nuclear Engineering, Seoul National University, Republic of Korea,
[2]Korea Atomic Energy Research Institute, Daedeok-daero,
Yuseong-gu, Daejeon, Republic of Korea

Abstract

Highly radioactive isotopes remain within spent nuclear fuels even one million years after discharge from the reactors. To resolve this problem in a manageable period, pyroprocessing has been explored to achieve sufficient throughput with inaccessible high temperature and strong radiation. Such remote operations, especially at uranium electrorefining, are challenges for repeated experiments that also generate a pile of radioactive wastes. Computational analysis is a plausible option to reduce trials and errors to find optimised designs and operating conditions of the electrorefiner.

To allow simulations to replace electrorefining experiments as much as possible, a three-dimensional multi-species electrochemical model has been developed. Commercial computational fluid dynamics software was coupled with user-defined electrochemical modules. Ion transport equation governs overall mass transport and concentration distribution while concentration-modified Butler–Volmer equation controls electrochemical reactions at electrodes. This model was already validated by molten salt electrorefining experiments using EBR-II spent fuels in co-operation with the Idaho National Laboratory. At that time, we benchmarked 80 hours long variations of overall cell potential only due to a lack of position-dependent information. Thus, it is needed to examine the model's capability to predict position-dependent potential and current. Here, we further validated the model with well-proven aqueous systems which experimentally measured more specific results other than cell potential. Cu-Ni co-depositions in $CuSO_4$ and $NiSO_4$ solution were experimented using both a corrosion cell and a rotating cylindrical hull cell. First, transfer coefficients, exchange current densities, and other materials properties of Ni^{2+} and Cu^{2+} in sulphate solution were estimated by cathodic potentiodynamic polarisation at the static corrosion cell. Second, the co-deposition experiment was galvanostatically conducted without stirring in the corrosion cell. Third, the co-deposition was also tried in the rotating hull cell. Fourth, simulated cathodic overpotential changes were validated to measured results at the corrosion cell. Fifth, cathodic overpotential distributions at the hull cell were benchmarked with computational results, as a function of position, cathode rotating speeds, and applied current densities.

Benchmark tests at various operating conditions and two different geometries generally showed good agreement between simulations and experiments. Despite minor discrepancies at detailed potential variations, these could be improved using more accurate electrochemical properties and considering current efficiency, nucleation overpotential, and other missing effects. Therefore, the multi-species co-deposition model could be a computational design tool to predict current densities and overpotentials for electrorefiners.

Introduction

Long-living radioactive isotopes in spent nuclear fuels require safety assurance for up to one million years after discharge from the reactors in the U.S. [1]. To resolve this problem in a manageable period, pyroprocessing has explored to achieve sufficient throughput with inaccessible high temperature and strong radiation. Such remote operations, especially at uranium electrorefining, are challenges for repeated experiments that also generate a pile of radioactive wastes [2]. High-fidelity computational simulation can be a powerful means of process design and characterisation as well as an operation-aid option to reduce errors in the operations of an electrorefiner.

For this reason, a large number of electrorefining computational models including REFIN [3], PYRO [4], TRAIL [5], GPEC [6] and PRAGAMAN [7] have been developed. Each of these computational models can produce vital information for a pyro-electrochemical system. However, as the design of the electrochemical system evolves with complex structures to increase throughput, significant discrepancies are found when the simulation was compared with the experimental results. In earlier electrochemical reaction models, it was difficult to accurately simulate hydrodynamic effect and electrochemical reactions simultaneously. Since the mixing behaviour of the bulk solution determines ion transport in the boundary layers on the electrode surface, cathodic deposition rate varies widely in a complicated geometry. Therefore, hydrodynamic behaviour should be coupled with the electrochemical process in simulation in order to investigate local contamination on the cathode during electrorefining.

Authors have developed a three-dimensional numerical model for the electrodeposition system by utilising commercial computational fluid dynamic models, including ANSYS-CFX and CFD-ACE+. The computational models were set up to investigate local current density distribution along the cathode and applied potential change during electrorefining with a Mark-IV electrorefiner which has a complex geometry for use at Idaho National Laboratory (INL) to treat experimental breeder reactor-II (EBR-II) [8] [9]. To validate and demonstrate the accuracy of the developed model more thoroughly using well-defined experiments, copper and nickel electro-deposition experiments in an aqueous system were conducted in this work. The aqueous system was selected since it can be conducted with much greater sophistication and accuracy while retaining the physics of the prototype pyroprocesssystem. This paper described the method and results of the model validation including experimental and numerical simulation results on the polarisation experiment and overpotential distribution along the cathode in static cell and rotating cylindrical Hull (RCH) cell using copper sulphate and nickel sulphate.

Experiment

Static cell experiment

A static cell without stirring experiment was prepared to focus on the validation of the computational electrochemical reaction model. The static cell has a similar geometry to the geometry described in the ASTM Method G5-2004 year which is an anode polarisation experiment, as presented in Figure 1 [10]. Saturated calomel electrode (SCE) and graphite were used for the reference electrode and the counter electrode, respectively. A Cu rod was used for working electrode after surface polishing using grit 800 silicon carbide paper. The height of the working electrode is 12.7 mm and the diameter is 9.5 mm. In addition, to reduce oxygen concentration in the solution, gas

bubbling using mixture gas of argon and 4% hydrogen was conducted. A litre of electrolyte with 1M $CuSO_4$ solution with pH of 4.0 and a conductivity of 0.05 S/cm was employed in each experiment. The temperature of the electrolyte was kept at 30±1°C throughout the experiment while cathodic polarisation curves were generated for Cu deposition.

Figure 1: Left: polarisation cell described in ASTM G5 (anode polarisation experiment) and Right: static cell used in this study

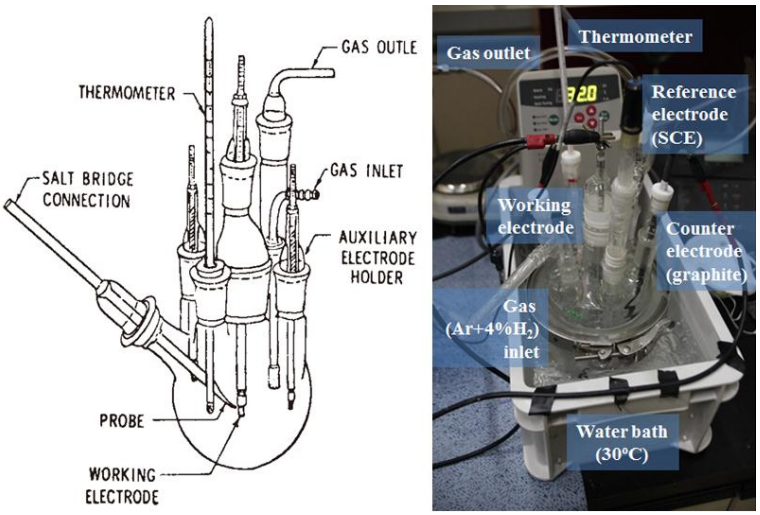

Rotating cylindrical hull (RCH) cell experiment

To validate the numerical model on the electrochemical hydrodynamic model, the RCH cell experiment was conducted. RCH cell has an advantage for the electrodeposition study because a wide range of current density on the working electrode could be investigated in a single experiment, as shown in Figure 2. RotaHull® cell geometry, which has been commercially fabricated, was used and it has been slightly changed to measure overpotential distribution along the cathode [11] [12]. Eight Luggin probes were connected with the Ag/AgCl reference electrodes through miniaturised solution bridges, as described in Figure 2. The cell consists of a rotating cylindrical working electrode made of Type 316 stainless steel or of Cu with a height of 8.0 cm and a diameter of 6.0 mm and a stationary platinum-titanium mesh anode with a height of 2.5 cm and a thickness of 1 mm positioned on the outer surface of a concentric cylindrical insulator with a 4.4cm inner diameter and 5.0 cm outer diameter, as shown in Figure 2.

All other supporting elements inside the cell were made of polytetrafluorethylene (PTFE) insulator. The aqueous solution for the RCH cell was made from 50 mM $CuSO_4$ and 500 mM Na_2SO_4. Na_2SO_4 was added as supporting electrolyte. The solution has a pH of 4.0 and a conductivity of 64 mS/cm at 25°C.

Using the RCH cell, both the polarisation experiment and galvanostatic experiments were conducted. Transfer coefficient, exchange current density, diffusion boundary layer thickness and equilibrium potential were obtained by curve-fitting potentiodynamic polarisation results. These data were used as the polarisation curve for the computational model and for the benchmarking of the galvanostatic experimental results. For the polarisation curve, the fourth reference electrode, which is located near the centre of the cathode, was used as a reference electrode. For the galvanostatic

experiment, all 8 reference electrodes were used with multi-channel recorder (e-Corder ED1621, eDAQ) to investigate overpotential distribution along the cathode axis.

Figure 2: Rotating cylindrical hull (RCH) cell used in this study

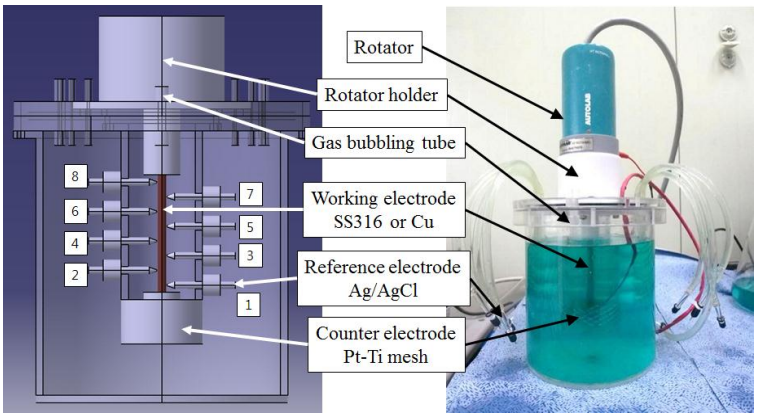

Numerical model

The electrochemical reaction rate is governed by the Butler-Volmer equation, as follows:

$$i = i_0[\exp(-\alpha \frac{nF}{RT}\eta) - \exp((1-\alpha)\frac{nF}{RT}\eta)] \tag{1}$$

where, i is current density, i_0 is exchange current density, α is transfer coefficient, n is the number of electrons evolved per reaction, F is Faraday constant, R is the universal constant, T is temperature in K and η is overpotential (=E- E_{eq}). Since the transfer coefficient is a multiplier on the overpotential and the electrochemical reaction rate is directly proportional to the exchange current density, it is crucial to use accurate parameters for the validity of a sophisticated modelling. These two parameters and the equilibrium potential (E_{eq}) could be obtained, in principle, by fitting the linear region of the experimental polarisation curve by Tafel Equation, as presented in Equation (2).

$$\eta = \frac{RT}{\alpha F}\ln i_0 - \frac{RT}{\alpha F}\ln i \tag{2}$$

However, in practice, it is hard to accurately determine the linear region because of ion concentration changes near the electrode surface with applied potential. For this reason, a modified Butler-Volmer Equation was used with the adjustment by concentration-dependent terms as presented in Equation (3):

$$i = i_0[\frac{C_0}{C_b}\exp(-\alpha \frac{nF}{RT}\eta) - \exp((1-\alpha)\frac{nF}{RT}\eta)] \tag{3}$$

where C_0 is surface concentration at the cathode and C_b is bulk concentration. Surface concentration at the cathode could be calculated from Fick's first law:

$$C_0 = C_b - \frac{i\delta}{nFD_0}\cdot \tag{4}$$

where δ is diffusion boundary layer thickness, and D_0 is diffusion coefficient.

By combining Butler-Volmer Equation and Fick's first law, a new equation can be introduced, as shown in Equation (5).

$$i = \frac{i_0[\exp(-\alpha \frac{nF}{RT}\eta) - \exp((1-\alpha)\frac{nF}{RT}\eta)]}{1 + \frac{i_0 \delta}{nFD_0 C_b}\exp(-\alpha \frac{nF}{RT}\eta)} \tag{5}$$

Diffusion boundary layer thickness does not change sensitively with concentration changes during a polarisation experiment. In addition, for the rotating cylindrical electrode at fully developed steady-state condition, diffusion boundary layer thickness is maintained at most locations except for those limited areas with vortices. Therefore, this equation can be used for fitting the polarisation curve to determine the exchange current density.

On this ground, Equation (5) is used to estimate electrochemical properties from the experimentally obtained polarisation curve. Since there are three unknown parameters in Equation (5), namely exchange current density, transfer coefficient and diffusion boundary layer thickness, the curve fitting with three variables was conducted using Matlab R2010 toolbox [13]. In this manner, transfer coefficients and exchange current densities for Cu and Ni in static cell and RCH cell were acquired, respectively. Obtained transfer coefficients and exchange current densities were used to simulate electrochemical reaction in both cells and obtained diffusion boundary layer thickness was compared to Eisenberg Equation developed to predict diffusion boundary layer thickness, δ, for the system with rotating concentric cylindrical geometry as represented in Equation (6) [11].

$$\delta = 12.64 d^{0.3} \nu^{0.344} D^{0.356} U^{-0.7} \tag{6}$$

where, d is diameter of the rotating cylindrical electrode, ν is kinetic viscosity, D is diffusion coefficient and U is the surface speed of electrode.

In the electrochemical system, the mass transfer of ions from electrode to electrode can be expressed as a combination of electromigration, diffusion and convection, as shown in Equation (7) [14].

$$N = -zuFC\nabla\Phi - D\frac{C_b - C_0}{\delta} + Cv \tag{7}$$

Where, z is charge quantity of ion, u is mobility, Φ is electric field, v is velocity.

Boundary conditions for modelling are described in Figure 3. The anode, which is a counter electrode, was established as the electrical ground and the cathode, which is the working electrode, was established as current source as well as a mass sink, as shown in Equation (8). Insulating and no slip boundary conditions were applied to the other parts, as described in Equation (9).

$$\dot{m} = -\frac{i_{app} M}{nF} \tag{8}$$

$$\frac{\partial C}{\partial n} = \frac{\partial \Phi}{\partial n} = 0 \tag{9}$$

CFD-ACE+ was employed, which is a commercial computational multi-physics package for coupled handling of hydrodynamics, heat transfer, chemical reaction, electromagnetics, etc. It has been widely utilised for multi-dimensional simulation on an electroplating system [15]. The modelling in this study employed two-dimensional geometries for both the static cell and the RCH cell, as shown in Figure 3. Since chemical concentration has a steep gradient near the cathode surface, fine meshes with a

minimum mesh size of 10^{-7} m were necessary to investigate concentration profile and ion behaviour.

Figure 3: Mesh configurations and boundary conditions of static cell and RCH cell

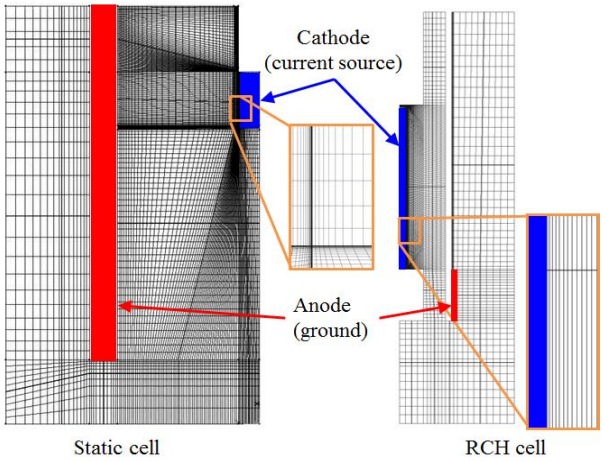

Results and discussion

Static cell

A cathodic polarisation curve on Cu electrodeposition in 1M CuSO4 solution was generated as represented as the black line in Figure 4. The curve was fitted by the equation combining Butler-Volmer Equation and Fick's first law, as shown in Equation (5). The voltage region below -0.8V was not utilised for generating the fitting curve since dendrite growth at the cathode was observed in this voltage region. Equilibrium potential was 0.067 V versus the saturated Calomel electrode. Transfer coefficient and exchange current density were obtained as 0.072 and 6.8 A/m^2. Diffusion boundary layer thickness was estimated at 10.64 µm. To verify the validity of estimated diffusion boundary layer thickness, it was compared to the diffusion boundary layer thickness estimated from computational modelling on the current density of 100 A/m^2. The diffusion boundary layer thickness calculated by the computational simulation was investigated about 11.24 µm, which is similar to the diffusion boundary layer thickness obtained from the fitting curve, 10.64µm as shown in Figure 4.

Figure 4: Mass fraction distribution of Cu^{2+} near cathode as calculated by the computational model

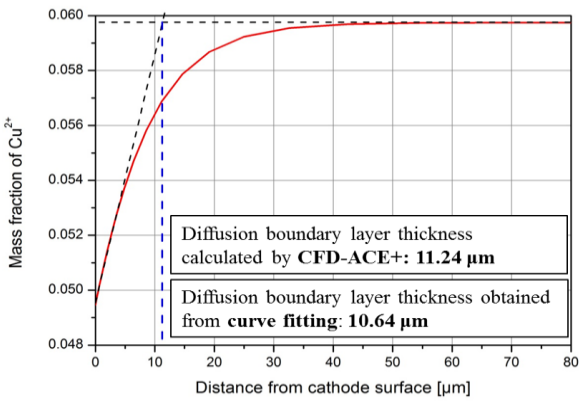

Using the obtained transfer coefficient and exchange current density, a polarisation curve was generated by the computational model, as presented in Figure 5. To reduce computational complexity, the polarisation curve was obtained by 12 steady state galvanostatic simulations with current densities of 100, 200, 400, 600, 800, 1 000, 1 200, 1 400, 1 600, 1 800, 2 000 and 3 000 A/m^2, respectively. The computationally regenerated polarisation curve, presented as the blue line in Figure 5, shows good agreement with the fitting curve except for both ends of the important potential range.

Figure 5: Comparison of polarisation curves obtained from the experiment (black line), the fitting curve using Equation 5 (red line) and computational simulation (blue line)

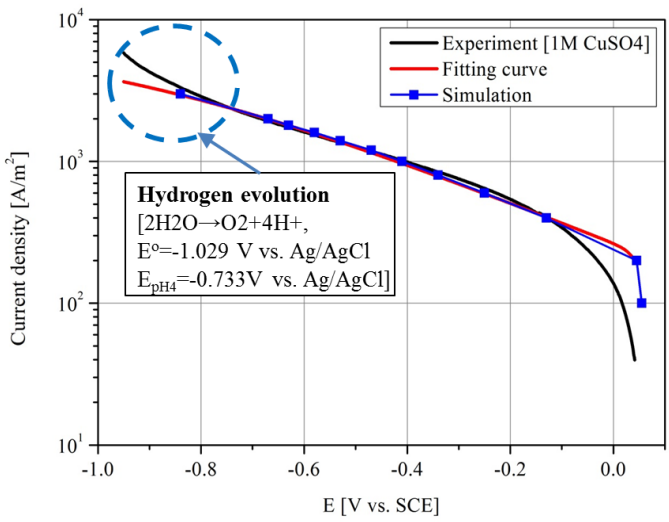

However, there are some discrepancies between the computational results and the experiment in the extreme potential regions. The differences are expected to have originated from the error in the electrochemical parameters estimated from the fitting curve. Therefore, to reduce the discrepancies, it is necessary to generate a more accurate fitting curve. Equation (5) is suitable for only single species electrodeposition. However, in the actual experiment, there could be a side reaction such as an inhibition reaction by cathode surface oxide, which can suppress a significant portion of total current density at the initial stage of the polarisation curve on copper electrodeposition. Increased current density at high cathodic overpotential is due to water decomposition effect.

RCH cell

A consistent approach was applied to the RCH cell experiment and for computational simulation. A polarisation curve on copper electrodepostion with the cathode rotating speed of 480 rpm was produced using forth reference electrode, as presented in Figure 6. Cu rod was used as cathode for the polarisation experiment. The voltage region below -1.2V was not used for generating the fitting curve since a bubble rise on the rotating cathode was observed. The bubble could be generated by the hydrogen generation reaction ($H_2O+2e \rightarrow H_2+OH^-$) whose potentials are -1.029 V versus Ag/AgCl reference electrode for the standard solution and -1.324 V versus Ag/AgCl reference electrode for the solution of pH 4. From the fitting curve, exchange current density was examined as 4.61 A/m^2 and transfer coefficient was obtained as 0.0783. It is noticeable that transfer coefficients from two totally different cells indicate similar values. Diffusion boundary layer thickness was estimated at 32.65 µm. It is 10µm smaller than the diffusion boundary layer thickness obtained from the Eisenberg Equation. The difference could occur because the Eisenberg Equation was established by experiment with length to

diameter ratios from 0.3 to 3, but the cathode used in this study has an h/d ratio of 13.3 [16].

Figure 6: Polarisation curve and the fitting curve on copper deposition in RCH cell with the cathode at a rotating speed of 480 rpm

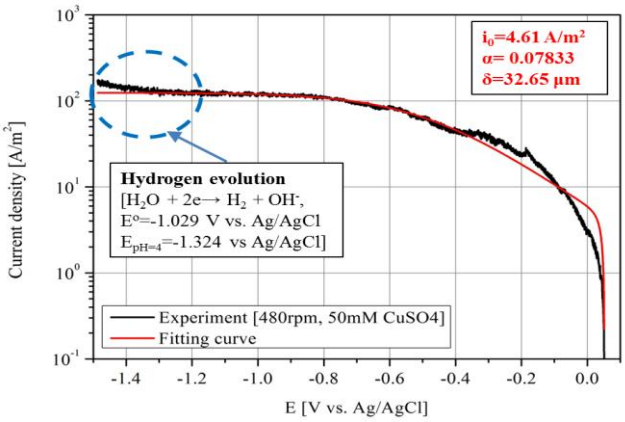

As part of verification of the computational model, overpotential distribution along the cathode was benchmarked for five average current densities, 2, 4, 6, 8 and 10 mA/cm^2 respectively, as shown in Figure 7. The position of x=0 indicates the nearest position of cathode from the anode. Overpotential distributions were measured by eight reference electrodes with Luggin probes. Since overpotentials were measured using reference electrodes, equilibrium potential for the system with 50 mM CuSO4 solution and Cu electrode was added to calculated overpotential. Across all applied current densities, calculated overpotentials are almost equivalent to measured overpotentials. Since the measured overpotentials had the noise level of about 50 mV, the discrepancies are within the noise level. If the noise level could be reduced, more detailed comparison could be conducted. In addition, discrepancies could be improved by using more accurate electrochemical properties and considering current efficiency, nucleation overpotential, and other missing effects.

Figure 7: Benchmark of computationally investigated overpotential distribution along the cathode against experimentally measured overpotential distribution: the position of x=0 is the nearest position of cathode from anode

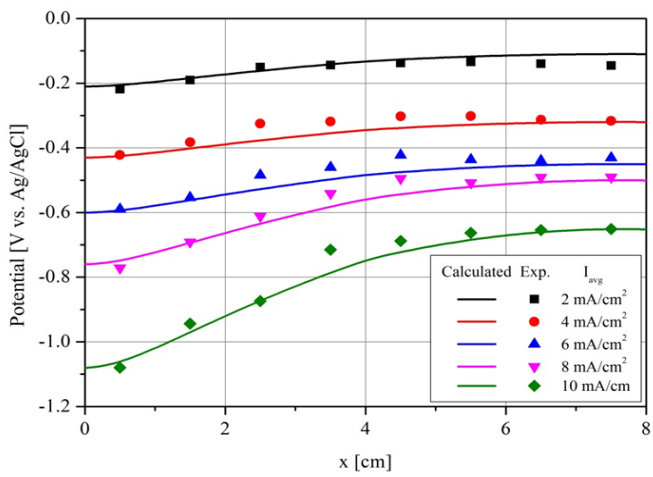

Conclusion

As part of the validation of the numerical electrochemical hydrodynamic model, benchmark studies of the polarisation curve on copper deposition in static cell and overpotential distribution along the cathode in RCH cell were conducted. To obtain exchange current density and transfer coefficient by fitting polarisation curve, the equation combining Butler-Volmer Equation and Fick's first law was driven. The polarisation curve for the static cell was regenerated by computational model using electrochemical properties obtained from curve fitting. The computationally regenerated polarisation curve is almost equivalent to the fitting curve on polarisation curve and there are no significant discrepancies from the experimentally obtained polarisation curve. In a similar manner, exchange current density and transfer coefficient were obtained for the RCH cell. Transfer coefficients obtained in the static cell and RCH cell are almost equivalent but exchange current densities are not because of the $CuSO_4$ concentration difference. With estimated exchange current density and transfer coefficient, overpotential distributions along the cathode according to applied current density were simulated. The numerically calculated distributions show almost the same distributions measured experimentally with discrepancies within the noise level. This study shows the possibility for the application of a numerical model to design and optimisation of an electrorefiner and electrochemical system. In the near future, after conducting more validation work including benchmark on various geometries and operating conditions, computational modelling could contribute to developing an innovative electrochemical process.

References

[1] J.J. Laidler, J.E. Battles, W.E. Miller, J.P. Ackerman, E.L. Carls (1997), "Development of Pyroprocessing Technology," *Progress in Nuclear. Energy*, 31, 131-140.

[2] J.B. Choi (2009), "Status of Fast Reactor and Pyroprocess Technology Development in Korea," *Proc. FR09*, 7-11 December 2009, Kyoto, Japan.

[3] B.G. Park (1999), "A Time-dependent Simulation of Molten Salt Electrolysis for Nuclear Wastes Transmutation", *Doctoral Thesis in Department of Nuclear Engineering*, Seoul National University, Seoul.

[4] J. Ackerman (1989), "PYRO, A System for Modeling Fuel Reprocessing," *Transactions of American Nuclear Society*, 60, 168-169.

[5] T. Kobayashi, M. Tokiwai (1993), "Development of TRAIL, a simulation code for the molten salt electrorefining of spent nuclear fuel," *Journal of Alloys and Compounds*, 197, 7-16.

[6] R.K. Ahluwalia, T.Q. Hua (2002),"Electrotransport of uranium from a liquid cadmium anode to a solid cathode," *Nuclear Technology*, 140(1), 41-50.

[7] S. Ghosh, B.P. Reddy, K. Nagarajan, P.R. Vasudeva Rao (2010), "PRAGAMAN: A Computer Code for the simulation of electrotransport during molten salt electrorefining," *Nuclear Technology*, 170, 430-443.

[8] S. Choi, I.S. Hwang (2011), "Uncertainty studies of real anode surface area in computational analysis for molten salt electrorefining," *Journal of Nuclear Materals*, 416 (3), 318-326.

[9] S. Choi, I.S. Hwang (2010), "Three-dimensional multispecies current density simulation of molten-salt electrorefining," *Journal of Alloys and Compounds*, 503, 177-185.

[10] ASTM (2004), "Standard Reference Test Method for Making Potentiostatic and Potentiodynamic Anodic Polarization Measurments," ASTM G5-94.

[11] C.T.J. Low, F.C. Walsh (2007), "Numerical simulation of the current, potential and concentration distributions along the cathode of a rotating cylinder Hull cell," *Electrochimica Acta*, 52, 3831-3840.

[12] J. Park (2009), "Numerical simulation of a Rotating Cylindrical Hull cell using Two- and Three-dimensional Electrorefining Models," *Proc. Global* 2011, 11-16 December 2011, Makuhari, Japan.

[13] MATLAB R2010a, the MathWorks™, (2010).

[14] A.J. Bard, L.R. Raulkner (2000), "Electrochemical Methods," Wiley.

[15] G. Ritter, T. Ritzdorf (2000), "Two- and three-dimensional numerical modeling of copper electroplating for advanced ULSI metallization," Solid-State Electronics, 44, 797-807.

[16] N. Simon, T. Flament (1995), "Determination of the diffusion coefficients of iron and chromium in Pb17Li," *International Journal of Heat and Mass Transfer*, 38 (16), 3085-3090.